International Journal of Biological Macromolecules 204 (2022) 587–592

Contents lists available at ScienceDirect

International Journal of Biological Macromolecules

journal homepage: www.elsevier.com/locate/ijbiomac

Micronized cellulose from citrus processing waste using water and electricity only

Samar Al Jitan [a], Antonino Scurria [b], Lorenzo Albanese [c], Mario Pagliaro [b], Francesco Meneguzzo [c], Federica Zabini [c], Reem Al Sakkaf [a], Ahmed Yusuf [a], Giovanni Palmisano [a,*], Rosaria Ciriminna [b,*]

[a] Department of Chemical Engineering, Center for Membranes and Advanced Water Technology, Research and Innovation Center on CO2 and Hydrogen, Khalifa University of Science and Technology, P.O. Box 127788, Abu Dhabi, United Arab Emirates
[b] Istituto per lo Studio dei Materiali Nanostrutturati, CNR, via U. La Malfa 153, 90146 Palermo, Italy
[c] Istituto per la Bioeconomia, CNR, via Madonna del Piano 10, 50019 Sesto Fiorentino (FI), Italy

ARTICLE INFO

Keywords:
Biocompatible polymer
Microcrystalline cellulose
Hydrodynamic cavitation
Citrus processing waste
CytroCell

ABSTRACT

Along with a water-soluble fraction rich in pectin, the hydrodynamic cavitation of citrus processing waste carried out in water demonstrated directly on semi-industrial scale affords an insoluble fraction consisting of micronized cellulose of low crystallinity ("CytroCell"). Lemon and grapefruit CytroCell respectively consist of 100–500 nm wide cellulose nanorods, and of 500–1000 nm wide ramified microfibrils extending for several μm. These findings establish a technically viable route to low crystallinity micronized cellulose laying in between nano- and microcellulose, using water and electricity only.

1. Introduction

Called "ageless bionanomaterial" by Dufresne [1], nanocellulose is a nanoscale material consisting either of cellulose nanocrystals (CNCs, also called nanocrystalline cellulose) or cellulose nanofibers (CNFs, also named nanofibrillated cellulose) having exceptional chemical, mechanical, biological, optical and thermal properties [2]. Potential applications range from transparent and foldable material in flexible energy and electronic devices [3], through carmaking using nanocellulose-reinforced polymer composites [4]. Being biocompatible, chemically stable and hydrophilic, nanocellulose also has numerous potential biomedical usages [5].

Large-scale production of this versatile biomaterial so far has been limited by the demanding physical and chemical conditions, required first to separate the lignin from wood lignocellulosic biomass, and then to extract nanocellulose from the latter cellulosic fraction [1,2]. Following the separation step using either acid-chlorite or alkaline treatment (and thus generating large amounts of wastewater), nanocellulose is generally extracted via acid hydrolysis (adding to the wastewater burden), steam explosion (with high energy consumption), enzymatically (requiring overly long extraction times), mechanically (high pressure homogenization, and ball milling methods) or by ultrasonication, with large energy demand [2].

Comprised of highly crystalline cellulose I only, CNC consists of whisker shaped nanocrystals (typically comprised of about 25 chains of 13,000 glucose units) 100–200 nm × 5–10 nm (low length/diameter aspect ratio between 10 and 100) [6]. The material has a tensile strength similar to that of aramid-fiber (10 GPa), and it is usually produced via acidic hydrolysis of plant cellulose pulp. Its suspensions have liquid-crystalline properties. The industrial production of CNC from wood cellulose pulp using sulphuric acid has an estimated production cost ranging from $3632/t to $4420/t, with feedstock cost and capital investment being the major cost drivers [7]. Yet, in the same year of these detailed estimates (2017) for large scale production, CNC was reported to be sold at $1000/kg [8].

CNF has a high aspect ratio (length/diameter = 100–150), includes amorphous cellulose along with cellulose I, and is produced via mechanical processes (homogenization, sonication or steam explosion). Its dispersions in water exhibit gel-like characteristics.

In 1998, Isogai and Sato successfully applied de Nooy's polysaccharide selective oxidation process [9] to partly convert the primary alcohol groups of regenerated and mercerized cellulose to carboxylates using catalytic amounts of 2,2,6,6-tetramethylpiperidine-1-oxyl (TEMPO) and NaBr with aqueous NaOCl as primary oxidant [10].

* Corresponding authors.
E-mail addresses: giovanni.palmisano@ku.ac.ae (G. Palmisano), rosaria.ciriminna@cnr.it (R. Ciriminna).

https://doi.org/10.1016/j.ijbiomac.2022.02.042
Received 13 December 2021; Received in revised form 3 February 2022; Accepted 8 February 2022
Available online 11 February 2022

Eight years later, the team in collaboration with Vignon discovered that native celluloses could be fibrillated in 3–5 nm nanofibrils by simple mechanical homogenization of the solution containing the TEMPO-oxidized cellulose [11]. The electrostatic repulsions between the cellulose fibrils bearing the carboxylate groups cause the shear and dispersion of the nanofibrils under mechanical agitation.

Since 2017, the process is used by a large paper company in Japan to manufacture CNF in the form of nano-dispersed fibers with uniform fiber width of 3 to 4 nm starting from bleached wood pulp at two different paper mills [12]. The company supplies the ingredient to different industrial customers producing CNF-reinforced tires, paper barrier cups for beverages, personal care, hygiene, and cosmetic products.

Currently, CNF is sold at a cost of $90–100/kg [13]. This cost is due both to the high cost of TEMPO as well as of disposal of the spent hypochlorite dilute solution containing the TEMPO catalyst which is lost in the process wastewater. Furthermore, TEMPO is a genotoxic ingredient [14] whose concentration in any material suitable for biomedical use, must be lower than a low threshold of toxicological concern (i.e., 4 ppm) [15]. In order to lower production costs, cellulose feedstocks alternative to wood pulp have been widely explored. Available in over 100 million tonne yearly amount, citrus processing waste (CPW) obtained from the orange, lemon and grapefruit juice processing industry would be an ideal feedstock.

Unfortunately, the routes to citrus nanocellulose starting from CPW based on enzymatic [16], microwave-assisted hydrothermal treatment [17], and acid hydrolysis [18], present technical limitations. For example, the nanocellulose fibrils obtained via multi-step microwave-assisted extraction of dried depectinated orange peel are deeply colored in brown due both to caramelized sugars and to the Maillard reaction between sugars and residual proteins at the high working temperatures required for extraction (120 °C to 180 °C) [17].

Now, we report that the “CytroCell” [19] insoluble fraction obtained along with a water-soluble fraction rich in pectin via the hydrodynamic cavitation of citrus processing waste carried out in water only consists of micronized cellulose of low crystallinity laying in between nano- and microcellulose. The “IntegroPectin” [20] citrus pectin extracted in the aqueous phase is highly soluble in water and is not found in the water-insoluble fraction.

2. Experimental

Obtained as described elsewhere [19,20] by processing >30 kg of citrus (lemon or grapefruit) industrial processing waste (from fruits organically grown in Sicily) in 120 L tap water, the “CytroCell” samples were simply isolated by filtration of the aqueous suspension resulting from the HC-assisted extraction.

After filtration, the solid CytroCell residue was mildly dried in an oven at 40 °C. Samples consisting of yellow (in the case of lemon) or pink (in the case of grapefruit) CytroCell with a delicate citrus scent were readily isolated. No further treatment was necessary beyond manual removal of a few lignin particles visually identified amid the CytroCell fibers in a glass Petri dish.

The transmission electron microscopy (TEM) analysis was performed by using a Tecnai G2 microscope operating at 200 kV. The TEM sample was prepared by suspending a very small amount of cellulose sample in deionized water, treating with ultrasounds, and finally depositing 5 μL of the diluted suspension on a 400-mesh Cu grid provided by Ted Pella (Redding, CA, USA). The solvent was evaporated at room temperature overnight. ImageJ image processing open source program was used for the analysis of the sample dimensions.

The thermogravimetric and differential thermal analyses (TGA/DTA) were performed using a Netzsch STA 449 F3 Jupiter thermal analyzer (NETZSCH-Gerätebau, Selb, Germany) using samples of ca. 13 mg. The temperature was increased from 25 °C to 700 °C at a constant heating rate of 10 °C/min under N_2 flow.

The zeta potential was measured with a Zetasizer Nano ZS analyzer (Malvern Panalytical, Malvern, Great Britain) using a laser wavelength of 633 nm. Measurements were carried out in a DTS1070 cell on a suspension of CytroCell (10 mg) in 1 L ultrapure (milli-Q) obtained using a Smart2Pure water purification system (Thermo Fisher Scientific, Waltham, MA, USA) water. The pH of the suspension was adjusted using 0.3 M HCl and 0.5 M NaOH.

Adsorption-desorption isotherms were determined using the a NOVA 2000e surface area and pore size analyzer (Quantachrome, Boynton Beach, FL, USA) with cryogenic N_2 as adsorbate. The CytroCell samples were first degassed under vacuum at about 110 °C overnight. The specific surface area of samples was determined using the multipoint Brunauer-Emmett-Teller (BET) model, using the average adsorption and desorption values of P/P_o in the range 0–0.35. The pore size distribution was calculated using the adsorption curve for all ranges of P/P_o by using the Barrett-Joyner-Halenda (BJH) model.

A Quanta 250 FEG scanning electron microscope (SEM) equipped with ETD detector (Thermo Fisher Scientific, Waltham, MA, USA) was used to study the morphology of the cellulose samples. A small fragment of each sample was deposited on a carbon tape attached to the stainless-steel stub to be loaded into the SEM using the stub holder. Each sample was sputter-coated with a thin layer (~10 nm) of gold as a conductive material to enhance the quality of the resulting images.

3. Results and discussion

Fig. 1 displays the TEM images of lemon CytroCell at two different degrees of magnification. The material is comprised of 0.5–3 μm long cellulose microfibrils whose section varies between about 110 and 420 nm (Fig. 1, bottom). The TEM photographs for grapefruit CytroCell in Fig. 2 display a different nanostructure consisting of ramified microfibrils whose diameter varies from 500 nm to 1 μm. Although the

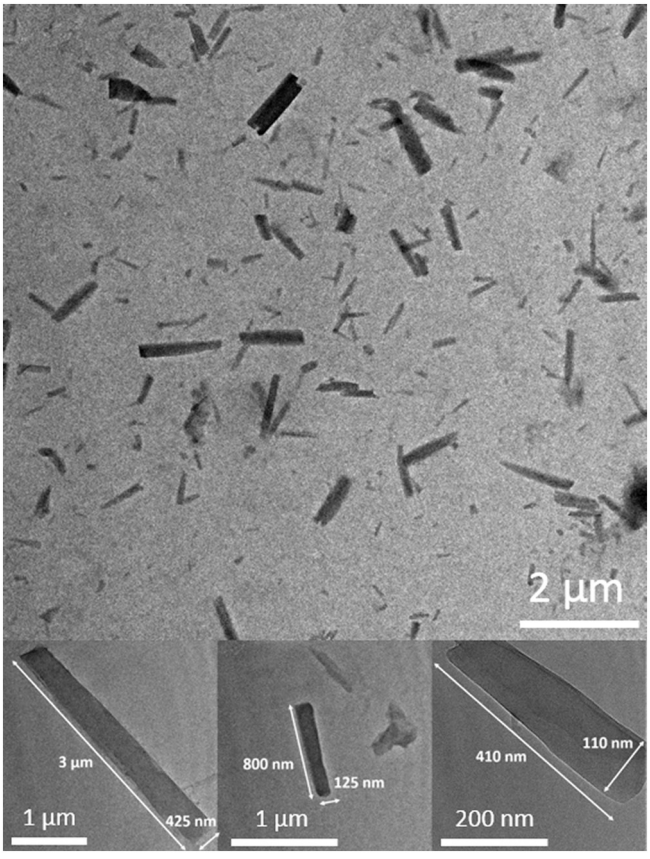

Fig. 1. TEM images of lemon CytroCell (*top*) and after focusing on selected single fibrils (*bottom*).

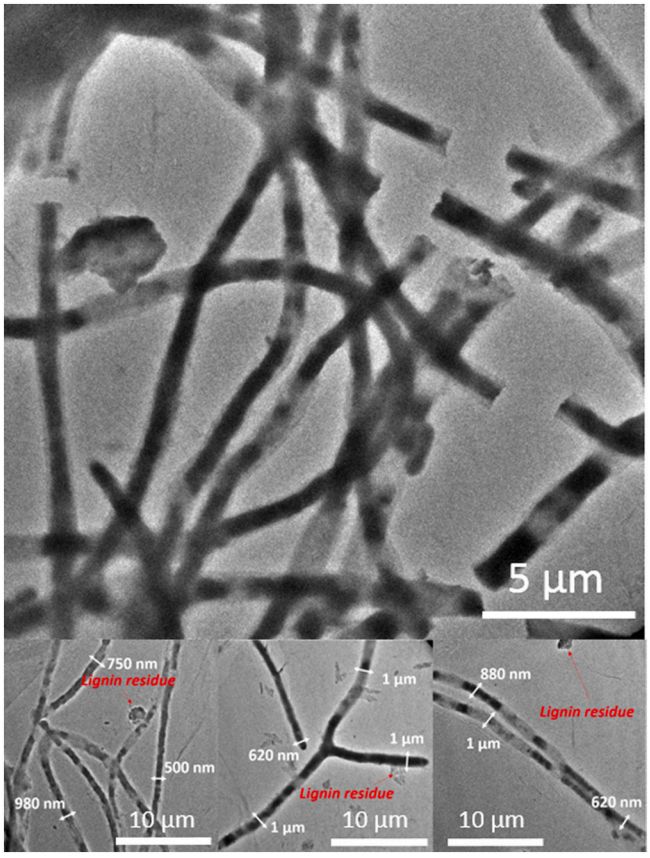

Fig. 2. TEM images of grapefruit CytroCell (*top*) and after focusing on selected single fibrils (*bottom*).

material is mainly composed of cellulose microfibers, some residual amorphous matter (possibly lignin) was detected from the TEM image at higher magnification (red arrows in bottom of Fig. 2), similar to what has been reported elsewhere [17].

The crystalline structure of the samples was determined by an XRD PANalytical Empyrean diffractometer, with a Cu Kα radiation of 1.54 Å, a scan step-size of 0.0167° and a 2θ scan range of 5–40°. The XRD measurements (plots shown in the Supplementary Information) confirmed previous XRD analysis showing that both CytroCell materials consist of cellulose of low crystallinity index (0.33 for lemon and 0.36 for grapefruit CytroCell) [21]. Again, the grapefruit-derived cellulose was found to contain more calcium oxalate crystals (with diffraction peaks at about 14.6°, 24.4° and 29.3°), abundant in both the lemon and grapefruit fruit peel [22]. Particularly abundant in plants grown in dry climates such as that of southern Sicily, from where both citrus fruits used to produce CytroCell originate [19,20], oxalate under drought conditions decomposes releasing CO_2 and water molecules [23].

We ascribe the fact that nanocellulose extracted from lemon CytroCell has a rod-like structure, while the nanocellulose extracted from grapefruit CytroCell has a "noodle-like" structure to the far higher amounts of citric acid present in waste lemon peel when compared to waste grapefruit peel. The higher acidity in the cavitation bubbles in the case of lemon-derived biowaste promotes breakage and hydrolysis of the cellulose fibrils.

The SEM images of both lemon and grapefruit CytroCell show (Fig. 3) a compact and relatively convoluted surface for both lemon nanocellulose nanorods and grapefruit nanocellulose microfibrils. These are the surfaces interacting with probe molecules such as the N_2 molecules during the surface area and pore size cryogenic measurements, or with the H_2O molecules when immersed in water. We briefly remind that these nanocelluloses adsorb and retain 8 g_{water}/g_{cell} in the case of lemon

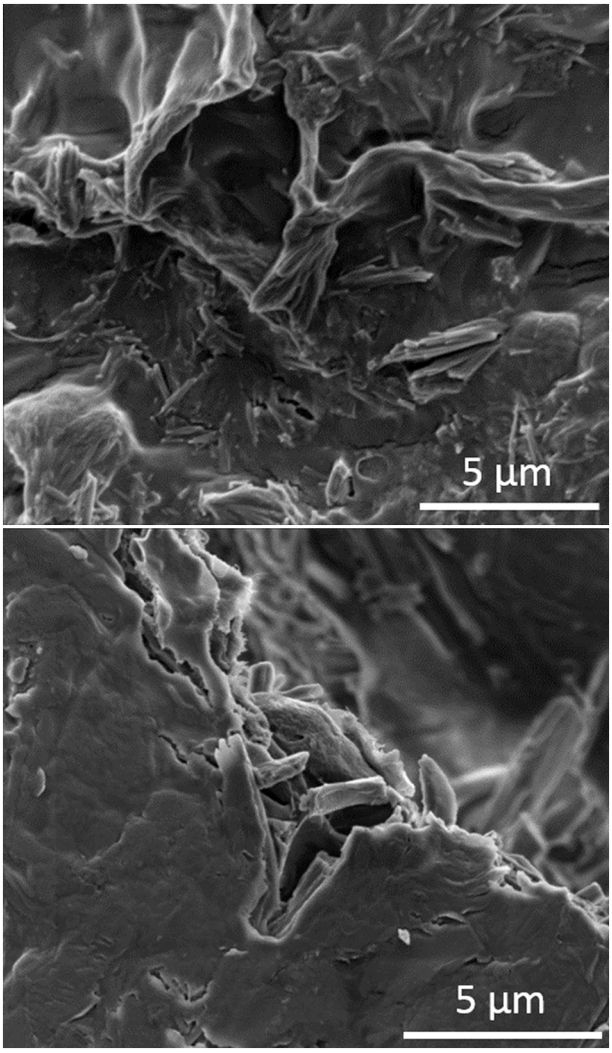

Fig. 3. SEM images of lemon (*top*) and grapefruit (*bottom*) CytroCell.

CytroCell and 5 g_{water}/g_{cell} for grapefruit CytroCell [19]. In general, for powdered and highly purified wood cellulose used as dietary fiber, the water holding capacity (WHC) increases with increasing fiber length [24].

The fact that the WHC of lemon nanocellulose of significantly shorter fiber length is higher than that of grapefruit nanocellulose suggests a different chemical composition of lemon CytroCell nanocellulose. Based on the IR analysis, this difference has been ascribed to the partial esterification of lemon CytroCell and the primary alcohol groups with citric acid residual in the wet lemon processing biowaste during the HC-assisted extraction [19].

The difference in the amount of water adsorbed in the native materials is noted also in the thermogravimetric analysis/differential scanning analysis (TGA/DTA) profiles of the two materials displayed in Fig. 4. The first weight loss around 100 °C corresponding to evaporation of bound water in cellulose is higher for lemon CytroCell, whereas the onset of thermal degradation at 42 °C occurs occurs at 5 °C lower temperature when compared to grapefruit nanocellulose (47 °C). The TGA and DTA profiles until the maximum degradation temperature (340 °C for lemon and 337 °C for grapefruit) are very similar, with two peaks, one near 240 °C and another near 340 °C. Based on recent thermal stability analysis of different nanocelluloses [25], the first peak is ascribed to the decomposition of negatively charged carboxyl groups on the fibril surfaces introduced by reaction with residual citric acid, whereas the second is assigned to pyrolysis of cellulose.

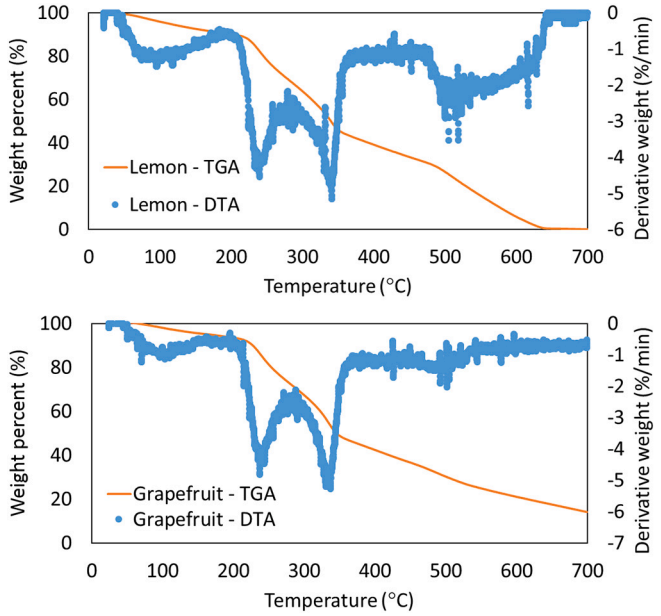

Fig. 4. TGA and DTA curves for lemon (*top*) and grapefruit (*bottom*) CytroCell.

The higher amount of carboxylate groups in lemon-derived CytroCell (visible in the IR spectra) [19] is reflected in the additional weight loss slope variation in the TGA and peak in the DTA profile at around 500 °C, which likely corresponds to the decomposition of the glycosyl-units resulting from the previous decomposition of the citric acid-esterified groups, followed by the formation of a carbonaceous residue.

Using a different porosimeter (Quantachrome NOVA 2000e) equipped with different burette when compared to that using the Micromeritics ASAP 2020 Plus used in previous surface area and pore size measurements, we were able to measure the adsorption-desorption isotherms of the free (i.e. non-aggregated powder) samples as originally reported [19]. In the latter case, the high electrostatic charge on the surface of both nanocelluloses allowed to use only monoliths rather than powders to carry out the N_2 adsorption experiments. The new experiments using the free powders returned a very similar pore size of 1.64 nm and 1.69 nm for lemon and grapefruit CytroCell, confirming that these new celluloses are mesoporous materials. The corresponding 24 and 27 nm pore sizes previously reported for the aggregate material [19], describe the porosity of nanocellulose aggregates.

For each citrus nanocellulose, the experimental zeta potential values showed large standard deviation values, particularly at neutral and alkaline pH (Fig. 5). These large variations may be due to fibrillar structure of both CNF samples made progressively less stable by the addition of base.

The zeta potential of lemon CytroCell at neutral pH measured several months after storage at room temperature, was slightly lower in absolute terms (−25 mV) that measured for the freshly obtained sample (−29.5 mV) [19]; whereas that of grapefruit CytroCell (−32 mV) was significantly larger than that of freshly obtained (−22.67 mV) grapefruit nanocellulose [19]. What is further relevant in light of forthcoming practical applications is that the zeta potential varies at relatively slow pace over a wide range of pH values between pH 4 and 13, starting to change at higher rate only at pH ≤3.

This behavior is similar to that of nanocellulose obtained in the form of CNC upon hydrolysis of wood pulp with sulphuric acid [26]. In the latter case, varying the pH across a wide range from pH 2 to pH 10 had little effect on nanocrystalline cellulose ξ potential until pH 1, when complete protonation of the sulphate groups was observed. In the present case, complete protonation of the bound citrate groups occurs at pH ~2 for both nanocelluloses, with a significant decrease of the zeta potential noted at pH 4 for both nanocelluloses.

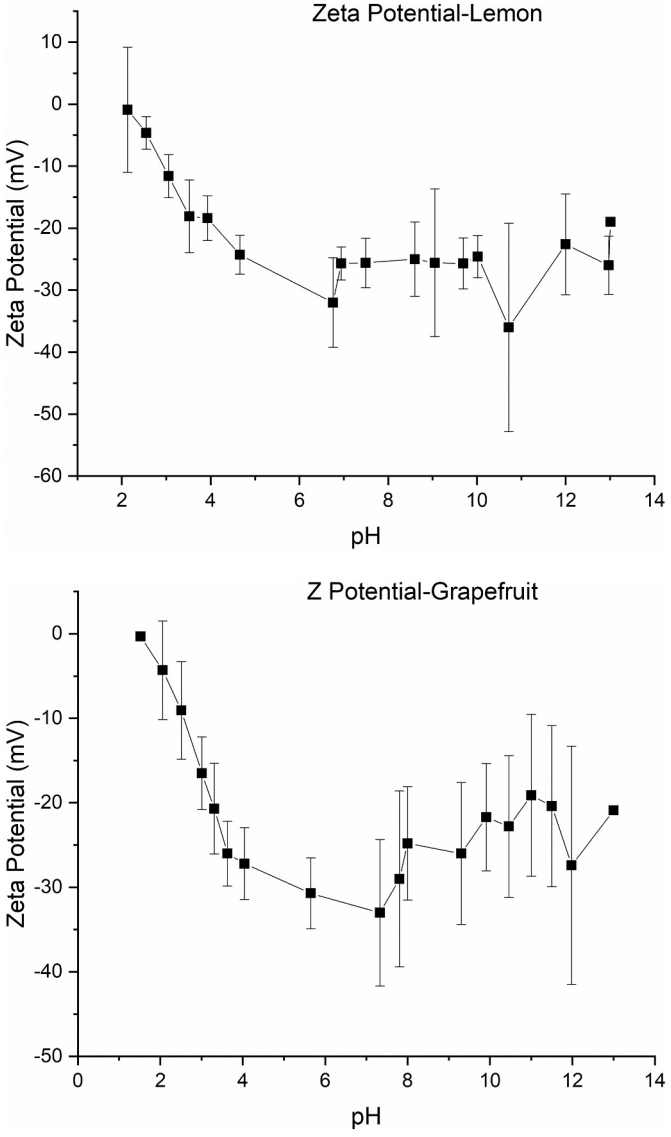

Fig. 5. Zeta potential at different pH for lemon (*top*) and grapefruit (*bottom*) CytroCell aqueous suspensions.

For both lemon and grapefruit samples, the zero charge point at pH 2.0 due to neutralization of the negative charge of the free carboxylate citrate groups by protons, depends on the pK_a of the bound citrate groups. Similar to what happens for bound sulphate groups for CNC extracted with H_2SO_4 [26], this finding, confirms that the carboxylate groups bound to the surface of both citrus nanocelluloses originate from citrate groups.

In 2010, Pandit and Pinjari in India were the first to report the outcomes of hydrodynamic and acoustic cavitation applied to a 1% *w/v* (0.5 kg in 50 L water) aqueous suspension of 63 μm cellulose microparticles [27]. Both forms of cavitation dramatically reduced cellulose crystallinity from 87% to 38%. The particle size was reduced to 1.36 μm and 0.3 μm for the hydrodynamically and ultrasonically processed cellulose samples, respectively. The thermal stability of the bulk microcrystalline cellulose was significantly reduced upon decrystallization and fibrillation, as shown by the melting point going from 101.78 °C for microcrystalline cellulose to 81.63 °C and 60.13 °C for the HC-derived and AC-processed nanocelluloses.

In this study, we show how hydrodynamic cavitation applied to citrus processing waste similarly affords micronized cellulose, starting from cellulose-rich renewable biowaste available worldwide in >100

million tonne yearly amount rather than from expensive pure cellulose microparticles.

4. Conclusions

In conclusion, we have discovered that the "CytroCell" [19] insoluble fraction obtained along with a water-soluble fraction, rich in pectin, via the hydrodynamic cavitation of citrus processing waste carried out in water only consists of micronized cellulose of low crystallinity laying in between nano- and microcellulose.

Directly carried out on a semi-industrial scale (>30 kg citrus biowaste in 120 L water), these micronized celluloses are readily obtained in large amounts through an efficient, one-pot process requiring no chemical reactant. Water is the only dispersion medium, and electricity is the unique energy form employed to run the cavitation process affording plentiful amounts of a biomaterial with numerous potential applications. Microcrystalline cellulose (MCC) is widely used by the pharmaceutical (as excipient, binder and adsorbent), food (as stabilizer, anti-caking agent, fat substitute, and emulsifier), beverage (as gelling agent, stabilizer and suspending agent), and cosmetic (as binder) industries, and has a huge application potential for producing MCC-based composite polymers for advanced applications in the automotive, biomedical and construction industries [28]. Commercially, it is produced via acid hydrolysis using an excess of H_2SO_4.

In the HC-based extraction process from citrus processing waste, no toxic or harmful effluents are generated during the extraction. The process is general and can be applied to any citrus fruit processing biowaste, including that resulting from orange juice production [29]. The safe and robust hydrodynamic cavitation process for the extraction of natural products, in conclusion, can be easily scaled-up [30]. A forthcoming study will demonstrate the economic viability of upscaling the process to convert citrus biowaste into valued micronized cellulose (and pectin) via controlled hydrodynamic cavitation.

CRediT authorship contribution statement

Samar Al Jitan, Reem Al Sakkaf, Ahmed Yusuf, Antonino Scurria, Lorenzo Albanese, Federica Zabini: Investigation, Visualization. Mario Pagliaro, Francesco Meneguzzo: Conceptualization, Writing- Original draft preparation. Giovanni Palmisano, Rosaria Ciriminna: Conceptualization, Supervision, Writing- Reviewing and Editing.

Data availability statement

All experimental data, including the results of nitrogen adsorption-desorption isotherms, are available by contacting the corresponding Authors.

Declaration of competing interest

The authors declare no conflict of interest. This research received no external funding.

Data availability

Data will be made available on request.

Acknowledgments

Thanks to OPAC Campisi (Siracusa, Italy) for kindly providing the lemon and grapefruit processing waste from which the lemon and grapefruit cellulosic materials were obtained. We thank Dr. Cyril Aubry, Khalifa University of Science and Technology, for assistance during the electron microscopy experiments.

Appendix A. Supplementary data

Supplementary data to this article can be found online at https://doi.org/10.1016/j.ijbiomac.2022.02.042.

References

[1] A. Dufresne, Nanocellulose: a new ageless bionanomaterial, Mater. Today 16 (2012) 220–227, https://doi.org/10.1016/j.mattod.2013.06.004.
[2] P. Phanthong, P. Reubroycharoen, X. Hao, G. Xu, A. Abudula, G. Guan, Nanocellulose: extraction and application, Carbon Resour. Convers. 1 (2018) 32–43, https://doi.org/10.1016/j.crcon.2018.05.004.
[3] O.A. Titton Dias, S. Konar, A. Lopes Leão, W. Yang, J. Tjong, M. Sain, Current state of applications of nanocellulose in flexible energy and electronic devices, Front. Chem. 8 (2020) 420, https://doi.org/10.3389/fchem.2020.00420.
[4] O. Adekomaya, Adaption of green composite in automotive part replacements: discussions on material modification and future patronage, Environ. Sci. Pollut. Res. 27 (2020) 8807–8813, https://doi.org/10.1007/s11356-019-07557-x.
[5] M. Jorfi, E.J. Foster, Recent advances in nanocellulose for biomedical applications, J. Appl. Polym. Sci. 132 (2015) 41719, https://doi.org/10.1002/app.41719.
[6] J.F. Rovol, L. Godbout, D.G. Gray, Solid self-assembled films of cellulose with chiral nematic order and optically variable properties, J. Pulp Pap. Sci. 24 (1998) 146.
[7] C. Abbati de Assis, C. Houtman, R. Phillips, E.M. Bilek, O.J. Rojas, L. Pal, M. S. Peresin, H. Jameel, R. Gonzalez, Conversion economics of forest biomaterials: risk and financial analysis of CNC manufacturing, Biofuels Bioprod. Biorefin. 11 (2017) 682–700, https://doi.org/10.1002/bbb.1782.
[8] B. Sithole, Roadmap towards innovation-driven forestry manufacturing, Biorefinery Industry Development Facility, Durban, South Africa, 4 October 2017 (accessed November 2, 2021), https://slideplayer.com/slide/13304284/.
[9] A.E. de Nooy, A.C. Besemer, H. van Bekkum, Highly selective nitroxyl radical-mediated oxidation of primary alcohol groups in water-soluble glucans, Carbohydr. Res. 269 (1995) 89–98, https://doi.org/10.1016/0008-6215(94)00343-e.
[10] A. Isogai, Y. Kato, Preparation of polyuronic acid from cellulose by TEMPO-mediated oxidation, Cellulose 4 (1998) 153–164, https://doi.org/10.1023/a:1009208603673.
[11] T. Saito, Y. Nishiyama, J.-L. Putaux, M. Vignon, A. Isogai, Homogeneous suspensions of individualized microfibrils from TEMPO-catalyzed oxidation of native cellulose, Biomacromolecules 7 (2006) 1687–1691, https://doi.org/10.1021/bm060154s.
[12] Nippon Paper Group, Cellulose nanofiber manufacturing technology and application development. https://www.nipponpapergroup.com/english/research/organize/cnf.html, 2021 (accessed November 2, 2021).
[13] M. Pagliaro, Cellulose nanofiber: an advanced biomaterial soon to become ubiquitous, Chim. Oggi 36 (4) (2018) 61–62.
[14] G. Szekely, M.C. Amores de Sousa, M. Gil, F. Castelo Ferreira, W. Heggie, Genotoxic impurities in pharmaceutical manufacturing: sources, regulations, and mitigation, Chem. Rev. 115 (2015) 8182–8229, https://doi.org/10.1021/cr300095f.
[15] H.E. Strohmeyer, G.W. Sluggett, Determination and control of TEMPO, a potentially genotoxic free radical reagent used in the synthesis of filibuvir, J. Pharm. Biomed. 62 (2012) 216–219, https://doi.org/10.1016/j.jpba.2011.12.036.
[16] M. Mariño, L.L. Da Silva, N. Durán, L. Tasic, Enhanced materials from nature: nanocellulose from citrus waste, Molecules 20 (2015) 5908–5923, https://doi.org/10.3390/molecules20045908.
[17] E.M. De Melo, J.H. Clark, A.S. Matharu, The hy-MASS concept: hydrothermal microwave assisted selective scissoring of cellulose for in situ production of (meso) porous nanocellulose fibrils and crystals, Green Chem. 19 (2017) 3408–3417, https://doi.org/10.1039/c7gc01378g.
[18] S. Naz, N. Ahmad, J. Akhtar, N.M. Ahmad, A. Ali, M. Zia, Management of citrus waste by switching in the production of nanocellulose, IET Nanobiotechnol. 10 (2016) 395–399, https://doi.org/10.1049/iet-nbt.2015.0116.
[19] A. Scurria, L. Albanese, M. Pagliaro, F. Zabini, F. Giordano, F. Meneguzzo, R. Ciriminna, CytroCell: valued cellulose from citrus processing waste, Molecules 26 (2021) 596, https://doi.org/10.3390/molecules26030596.
[20] D. Nuzzo, L. Cristaldi, M. Sciortino, L. Albanese, A. Scurria, F. Zabini, C. Lino, M. Pagliaro, F. Meneguzzo, M. Di Carlo, R. Ciriminna, Exceptional antioxidant, non-cytotoxic activity of integral lemon pectin from hydrodynamic cavitation, ChemistrySelect 5 (2020) 5066–5071, https://doi.org/10.1002/slct.202000375.
[21] A. Presentato, E. Piacenza, A. Scurria, L. Albanese, F. Zabini, F. Meneguzzo, D. Nuzzo, M. Pagliaro, D.F. Chillura Martino, R. Alduina, R. Ciriminna, A new water-soluble bactericidal agent for the treatment of infections caused by gram-positive and gram-negative bacterial strains, Antibiotics 9 (2020) 586, https://doi.org/10.3390/antibiotics9090586.
[22] R.L. Clements, Organic acids in citrus fruits. I. Varietal differences, J. Food Sci. 29 (1964) 276–280, https://doi.org/10.1111/j.1365-2621.1964.tb01731.x.
[23] G. Karabourniotis, H.T. Horner, P. Bresta, D. Nikolopoulos, G. Liakopoulos, New insights into the functions of carbon–calcium inclusions in plants, New Phytol. 228 (2020) 845–854, https://doi.org/10.1111/nph.16763.
[24] J.F. Ang, Water retention capacity and viscosity effect of powdered cellulose, J. Food Sci. 56 (1991) 1682–1684, https://doi.org/10.1111/j.1365-2621.1991.tb08670.x.
[25] I. Jankowska, R. Pankiewicz, K. Pogorzelec-Glaser, P. Ławniczak, A. Łapiński, J. Tritt-Goc, Comparison of structural, thermal and proton conductivity properties

of micro- and nanocelluloses, Carbohydr. Polym. 200 (2018) 536–542, https://doi.org/10.1016/j.carbpol.2018.08.033.
[26] R. Prathapana, R. Thapa, G. Garnier, R.F. Tabor, Modulating the zeta potential of cellulose nanocrystals using salts and surfactants, Colloids Surf. A Physicochem. Eng. Asp. 509 (2016) 11–18, https://doi.org/10.1016/j.colsurfa.2016.08.075.
[27] D.V. Pinjari, A.B. Pandit, Cavitation milling of natural cellulose to nanofibrils, Ultrason. Sonochem. 17 (2010) 845–852, https://doi.org/10.1016/j.ultsonch.2010.03.005.
[28] D. Trache, M.Hazwan Hussin, C.Tan Hui Chuin, S. Sabar, M.R.Nurul Fazita, O.F. A. Taiwo, T.M. Hassan, M.K.M. Haafiz, Microcrystalline cellulose: isolation, characterization and bio-composites application-a review, Int. J. Biol. Macromol. 93 (2016) 789–804, https://doi.org/10.1016/j.ijbiomac.2016.09.056.
[29] F. Meneguzzo, C. Brunetti, A. Fidalgo, R. Ciriminna, R. Delisi, L. Albanese, F. Zabini, A. Gori, L.Beatriz dos Santos Nascimento, A.De Carlo, F. Ferrini, L. M. Ilharco, M. Pagliaro, Real-scale integral valorization of waste orange peel via hydrodynamic cavitation, Processes 7 (2019) 581, https://doi.org/10.3390/pr7090581.
[30] D. Panda, S. Manickam, Cavitation technology - the future of greener extraction method: a review on the extraction of natural products and process intensification mechanism and perspectives, Appl. Sci. 9 (2019) 766, https://doi.org/10.3390/app9040766.